Detailed thermal, fire, and mechanical study of silicon-modified epoxy resin containing humic acid and other additives

ACS APPLIED POLYMER MATERIALS

pubs.acs.org/acsapm

Article

Detailed Thermal, Fire, and Mechanical Study of Silicon-Modified Epoxy Resin Containing Humic Acid and Other Additives

Virginia Venezia, Samuele Matta, Sandro Lehner, Giuseppe Vitiello, Aniello Costantini, Sabyasachi Gaan, Giulio Malucelli, Francesco Branda, Giuseppina Luciani,* and Aurelio Bifulco*

Cite This: *ACS Appl. Polym. Mater.* 2021, 3, 5969–5981

Read Online

ACCESS | Metrics & More | Article Recommendations | Supporting Information

ABSTRACT: Following a waste-to-wealth approach, humic acid (HA) was exploited as a flame retardant additive. The effect of its addition alone and in combination with urea (UR) and ammonium polyphosphate (APP) on the thermal, fire, and mechanical performances of a bisphenol A diglycidyl ether (DGEBA)-based epoxy resin modified with (3-aminopropyl)-triethoxysilane (AP) and cured with aliphatic isophoronediamine (IDA) has been investigated. Unlike in previous studies, a UL 94-V-0 classification was achieved for epoxy resin containing HA at 6 wt % and APP at only 1 wt % phosphorus (P) loading. The presence of silicon-modified epoxy chains ameliorated the distribution of the biowaste within the resin, and the addition of HA alone avoided melt dripping. Besides, APP and UR promoted a remarkable reduction (up to 52%) of the peak heat release rate (pHRR) values and a significant delay (up to 21%) of the time to ignition in cone calorimetry tests, and hence an increase (up to 1.8 min) of the time to flashover, without any detrimental effect on the overall mechanical behavior. The evolved gas, thermal, and fire analysis was used to propose the combined mode of action of HA, UR, APP, and silicon in the fire performance improvement of the hybrid epoxy system.

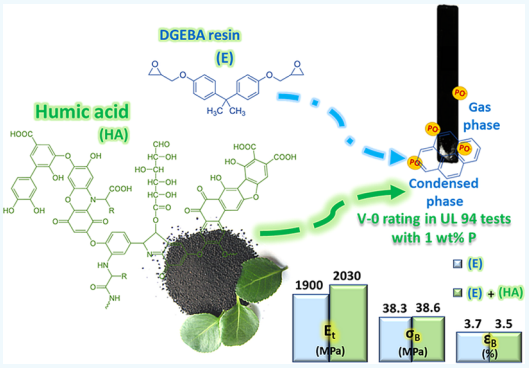

KEYWORDS: *humic acid, flame retardant, thermosetting polymer, biowaste valorization, bio-based additives, hybrid epoxy moiety*

1. INTRODUCTION

In recent years, human beings have been responsible for serious environmental impacts in terms of major environmental concerns related to global warming, depletion of natural resources, and increased waste production.[1,2] However, global awareness and governmental actions are now focused on a transition from a linear economic model toward a more sustainable circular approach, which allows for resources savings and waste reduction as well. Indeed, considering waste as a resource is mandatory to preserve human and environmental health, though, at the same time, it can provide a great opportunity for economic and technological growth.[3] Thus, worldwide, governments have been providing economic support for this transition through effective policies of intervention.[4] At the same time, the design and exploitation of more sustainable products, with a low impact on health and environment, have been attracting increasing interest from the scientific community. Recently, a huge production of biowastes has been recorded because of the human activities spanning from households to industrial applications, including food processing and biorefinery.[5] In the manufacturing of polymer-based products, some additives must be included to fulfill the physicochemical and mechanical performance requirements as defined by standards and regulations.[6] However, such compounds are mostly produced from nonrenewable sources and can give rise to serious ecological concerns mainly linked to the release of toxic species in the atmosphere.[7] This issue still poses huge limitations for the recycling of polymers.[3] Among polymer systems, epoxy resins are used to develop a large array of high-performance products, including linings and components in the aircraft sector, where, along with the typical requirements, severe fire safety standards and regulations must be fulfilled.[8] In this field, as greener alternatives than halogen-based flame retardants, halogen-free additives (e.g., ammonium polyphosphate (APP)), and bio-based and biomass-based raw materials (e.g., chitosan, lignin, cyclodextrins) have been investigated.[8] However, a noticeable amount of these compounds must be incorporated into the epoxy matrix to achieve satisfying fire performances. As an example, Zhang et al. prepared thermoplastic polyurethane composites through the addition of 6.25 wt % of chitosan derivatives (CSD) and 18.75 wt % of APP.[9] Further, extensive use of bio-based compounds can destroy the earth's regenerative capacity,

Received: September 18, 2021
Accepted: October 8, 2021
Published: October 18, 2021

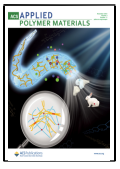

Table 1. Compositions of the Epoxy Samples

sample	E (g)	IDA (g)	HA (g)	AP (g)	UR (g)	APP (g)	P (%)	Si (%)
E	15	3.9						
E_12HA	15	3.9	2.3					
E_UR	15	3.9			0.8			
E_APP	15	3.9				0.8	1.3	
E_URAPP	15	3.9			0.8	0.8	1.3	
E_12HAUR	15	3.9	2.3		1.5			
E_12HAAPP	15	3.9	2.3			1.5	2.2	
E_12HAURAPP	15	3.9	2.3		1.5	1.5	2.1	
E12AP	15	3.9		2.3				1.4
E12AP_12HA	15	3.9	1.1	1.1				0.7
E12AP_UR	15	3.9		2.3	0.8			1.3
E12AP_APP	15	3.9		2.3		0.8	2.1	1.3
E12AP_URAPP	15	3.9		2.3	0.8	0.8	1.1	1.1
E12AP_12HAUR	15	3.9	1.1	1.1	0.8			0.6
E12AP_12HAAPP	15	3.9	1.1	1.1		0.8	1.1	0.6
E6AP_6HAURAPP	15	3.9	0.6	0.6	0.4	0.4	0.6	0.4
E12AP_12HAURAPP	15	3.9	1.1	1.1	0.8	0.8	1.1	0.6

giving rise to further environmental issues. Thus, in the context of sustainable development, the reuse of biowaste materials as functional flame retardant additives for polymer-based systems may represent one of the most promising approaches for moving toward a circular economy concept.[5,10] Among biowastes, humic acids (HAs) are the alkali-soluble fraction of natural organic matter obtained by the biological and chemical degradation of both vegetable and animal biomasses.[11] HAs consist of a skeleton of aliphatic or aromatic units, with a marked amphiphilic behavior. These moieties are stabilized by weak hydrophobic, hydrogen, and metal-bridged electrostatic bonds in supramolecular architectures that can change their functionalities depending on the chemical environment.[12] Due to the presence of oxygen-containing functional groups, a carbon-enriched chemical composition, and supramolecular architectures, HAs can promote the charring process during the epoxy degradation upon exposure to a flame or an irradiative heat flux, and can establish good physical interactions with the polymer matrix. Therefore, HAs can provide epoxy resins with a huge potential as flame retardants.[13] However, the use of HAs as effective flame retardants for polymer systems has been poorly investigated. Liu et al. chelated HAs with four different metal ions and incorporated them into a modified DGEBA resin to enhance its flame retardance. In particular, as a result of the incorporation of 10 wt % of HA-Fe and HA-Mn into the epoxy matrix, the limiting oxygen index (LOI) increased from 21.2% for pristine resin to 26.6 and 25.3%, respectively; meanwhile, the pHRR was reduced by 36 and 35.5%, respectively.[14] Despite HAs being used as a charring agent following Liu et al., as far as we know, no self-extinguishing materials using HA have been developed so far. Furthermore, a complete characterization of the mechanical and fire behavior of HA-containing epoxy systems is still missing, which is really needed to enable any technological exploitation. An excellent distribution of the flame retardants within the epoxy resin is crucial to achieve uniform overall performances. To this purpose, the reaction between DGEBA and (3-aminopropyl)-triethoxysilane can yield hybrid silicon-containing epoxy moieties can improve the interphase between the matrix and the filler, because of their capability to interact with polar and apolar components of the additives, hence enabling a fine dispersion.[15] Considering their amphiphilic nature, HAs are expected to achieve a very good distribution into silicon-modified epoxy resins and show promise towards obtaining enhanced charring behavior and fire performances.

In this study, a detailed study on the role of HA biowaste as a flame retardant for epoxy resin has been undertaken. To this purpose, hybrid silicon-modified epoxy composites were synthesized via the sol−gel procedure from DGEBA and AP and then cured with IDA as a cycloaliphatic hardener. HA, UR, and APP were added, alone or in combination, to this resin system in order to assess their role in flame retardance. Finally, a composite material with superior fire performance (V-0 rated in UL 94 tests) and low P-loading (not exceeding 1.0 wt %) was obtained. Then, the effect of P-N synergism on the flame retardance of the hybrid epoxy composites was investigated. Fourier-transform infrared spectroscopy with attenuated total reflectance (ATR-FTIR) was exploited for assessing the chemical composition consistency of the epoxy samples and the completeness of the reactions occurring between HA and both the epoxy sample and the curing agent. The thermal and fire behaviors of the obtained composites were thoroughly investigated by means of thermogravimetric analysis (TGA), differential scanning calorimetry (DSC), cone calorimetry, UL 94 vertical flame spread tests, and direct insertion probe-mass spectrometry (DIP-MS). Furthermore, the effect of various additives on the mechanical behavior of the epoxy resin was studied by three-point bending tests.

2. MATERIALS AND METHODS

2.1. Materials. (3-Aminopropyl)-triethoxysilane (AP, N98%), urea (ACS reagent, N99.0−100.5%), humic acid sodium salt (HA, technical grade), and ammonium polyphosphate (APP) were acquired from Sigma-Aldrich (St. Louis). Bisphenol A diglycidyl ether (DGEBA, SX10) and isophoronediamine (IDA, SX10) were purchased from MATES S.r.l. (Milan, Italy) and used as received.

2.2. Preparation of Hybrid Epoxy Composites. Pristine epoxy resin was prepared by following the procedure reported elsewhere.[16] Briefly, bisphenol-A-based epoxy resin (E, 15 g) was mixed with IDA (26 wt % of E) at room temperature, and then the resulting mixture was cured at 60 °C overnight, followed by post-curing at 80 °C for 4 h. In the preparation of epoxy composites (Table 1), AP was chosen as the coupling agent and exploited to improve the dispersion of HA

https://doi.org/10.1021/acsapm.1c01240
ACS Appl. Polym. Mater. 2021, 3, 5969−5981

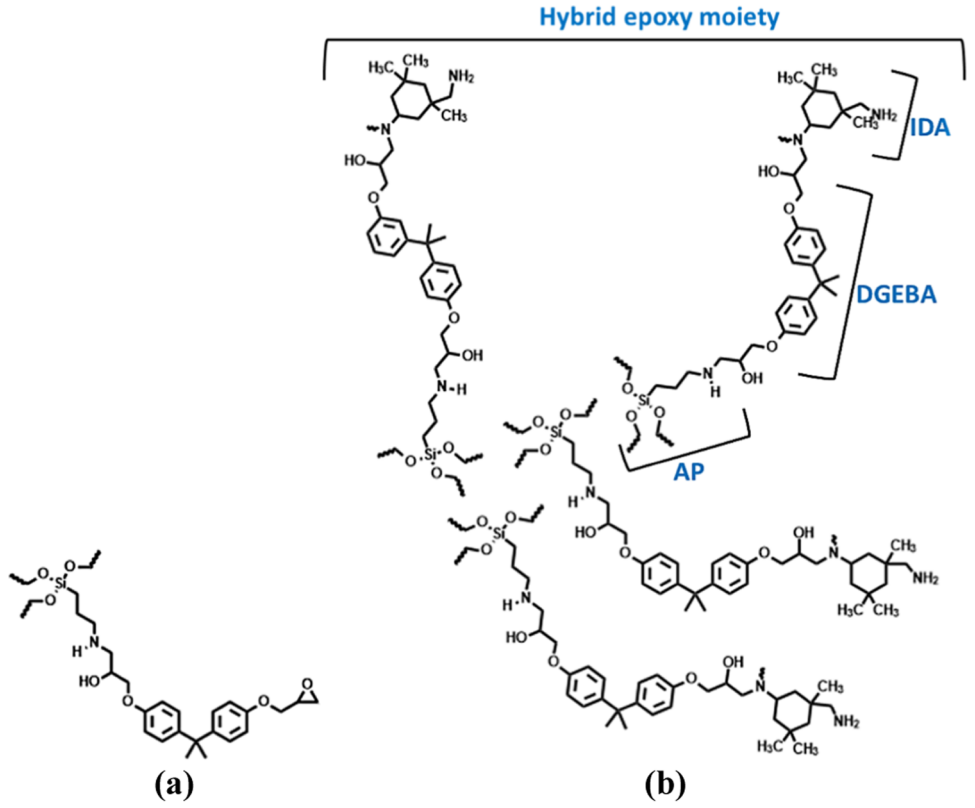

Figure 1. (a) Silanized epoxy species (i.e., AP-modified DGEBA epoxy chain); (b) hybrid epoxy moiety.

within the polymeric matrix. Samples containing AP were produced according to the following procedure:

- A specific amount of AP (6, 12 wt % of "E + IDA" mass) was added to E (15 g).
- The mixture was stirred at 80 °C for 2 h, followed by the addition of HA or HA/UR or HA/UR/APP with a fixed weight ratio, as reported in Tables 1 and S1.
- The mixture was kept for 90 min at 80 °C; then it was cooled down to room temperature before the addition of 3.9 g of hardener (IDA) and finally mixed for 5 min.
- The resulting system was cross-linked at 60 °C overnight and then post-cured (80 °C for 4 h).

The reaction between DGEBA and AP allows the formation of silanized epoxy species (Figure 1a), which may be generated via interaction of the $-NH_2$ groups of AP and oxirane rings of DGEBA. Silanized epoxy species result in hybrid epoxy moieties (Figure 1b) throughout the polymer matrix,[17−19] consisting of both polar (i.e., silane phase) and apolar (i.e., bisphenol A part) components. Therefore, in the presence of HA, due to its amphiphilic nature, these moieties may self-assemble in well-dispersed chemical structures,[15,20] accounting for a good distribution of HA into the apolar moieties.[1] Figure S1 shows the typical optical microscopy images of E12AP_HA, prepared by using AP and HA, and of E_HA, where the biowaste filler was directly added to the pristine polymer. It is evident that the use of AP was crucial to obtain a good dispersion of the filler, guaranteeing the reliability of the experimental results. The typical reaction batches are reported in Tables 1 and S2, together with the acronyms used throughout the paper.

2.3. Characterization. Fourier transformed infrared (FTIR) transmittance spectra were determined using a Nicolet 5700 FTIR spectrometer (Thermo Fisher, Waltham, MA) by means of a single-reflection attenuated total reflectance (ATR) instrument with a resolution of 4 cm^{-1} and 32 scans, and by exploiting the Thermo Scientific OMNIC Software Suite (v7.2, Thermo Fisher, Waltham, MA, 2005). The obtained spectra were normalized to the absorption bands at 1607 and 1509 cm^{-1}, attributable to the C=C bonds of the benzene rings present in the epoxy resin structure, to demonstrate that they do not further change after the curing reaction.

An EVO 15 scanning electron microscope (SEM) from Zeiss (Oberkochen, Germany), coupled to an Ultim Max 40 energy-dispersive X-ray (EDX) micro-analyzer by Oxford Instruments (High Wycombe, U.K.) with AZtecLive integrated software, was exploited to investigate the structure of the residual char after cone calorimetry (CC) combustion. Fragments of the compounds obtained by a brittle fracture were attached to conductive adhesive tapes and gold-metallized. The dispersion of HA in the epoxy matrix was assessed using a Wild M3Z binocular microscope with a resolution of 35−400× (Wild, Heerbrugg, Switzerland), coupled to an Olympus digital camera (Olympus, Tokyo, Japan).

Differential scanning calorimetry (DSC) tests were performed by means of a Q20 TA Instrument apparatus (New Castle, DE), using samples of about 8 mg stored in closed aluminum pans. The samples were first heated (from 0 to 150 °C at 10 °C/min) to remove their previous thermal history. Then, the materials were cooled (from 150 to 0 °C at −10 °C/min) and a second heating-up was carried out (from 0 to 150 °C at 10 °C/min). The temperature post the curing onset, temperature of the peak, and area were found on the first heating-up. T_g was calculated as the midpoint between the onset and end point of the inflectional tangents on the second heating-up curve.

The thermal behavior of the materials was investigated through thermogravimetric analysis (TGA), using a Q500 system from TA Instrument (New Castle, DE); the samples were heated from 50 to 800 °C at 10 °C/min, in nitrogen or air (gas flow: 60 mL/min). The tests were performed by placing about 10 mg of the sample in open alumina pans. $T_{5\%}$ and $T_{10\%}$ (temperatures at 5 and 10% of weight loss, respectively), T_{max} (temperature at which the maximum weight loss rate is observed in the dTG—derivative—curves), and residues were measured.

The flammability of all composites was assessed by UL 94 vertical flame spread tests (IEC 60695-11-10; sample dimensions: 13 × 125 × 3 mm^3).

The combustion behavior was studied by means of CC (Noselab Ats, Nova Milanese, Italy) according to the ISO 5660 standard, by

https://doi.org/10.1021/acsapm.1c01240
ACS Appl. Polym. Mater. 2021, 3, 5969−5981

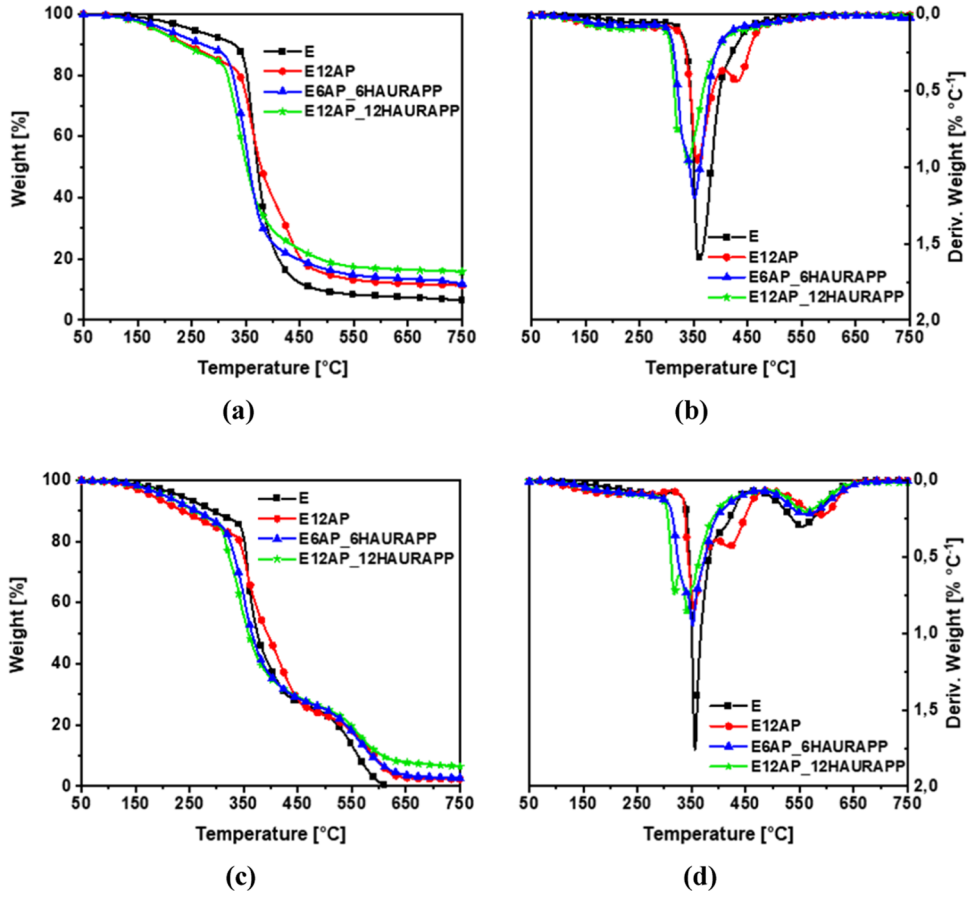

Figure 2. (a, c) TGA curves and (b, d) DTG curves of EPO and epoxy composites under N_2 (a, b) and air (c, d).

using squared samples (100 × 100 × 3 mm^3), with a heat flux of 35 kW/m^2, in horizontal configuration. Time to ignition (TTI, s), total heat release (THR, MJ/m^2), and peak of the heat release rate (pHRR, kW/m^2) were measured. The total smoke release (TSR, m^2/m^2) was also evaluated. For each sample, the experiments were repeated at least three times in order to ensure reproducible and significant data.

Direct inlet probe-mass spectroscopy (DIP-MS) was performed with a Finnigan/Thermoquest GCQ ion trap mass spectrometer (Austin, TX) equipped with a DIP module. Approximately 1 mg of the sample was placed in a quartz cup located at the tip of the probe and inserted into the ionization chamber operated at 70 eV ionization voltage; the temperature of the ionic source was set at 200 °C and the pressure was below 10^{-6} mbar. The probe temperature was varied from 30 to 450 °C at 50 °C/min.

Dynamic mechanical analysis (DMA) was conducted by means of a Q800 TA Instrument (New Castle) in single-cantilever configuration, on rectangular specimens (35 mm × 10 mm × 4 mm of length × width × thickness, respectively), to measure the storage (E') and loss moduli versus temperature. The investigated systems were submitted to the following ramp-up of temperature: from 30 to 150 °C, at 2 °C/min and 1 Hz of frequency.

Tensile tests were performed using a Zwick Z100 dynamometer (ZwickRoell S.r.l., Genova, Italy), following the ASTM D638 standard, on rectangular specimens (50 × 10 × 4 mm^3), using a 100 kN load cell at 1 mm/min rate until 0.2% deformation was reached. Then, the rate was increased up to 10 mm/min until the specimen broke. Five specimens were tested for each formulation, and the average values of the tensile modulus (E_t), the elongation at break (ε_B), and the tensile strength (σ_B) were calculated.

3. RESULTS AND DISCUSSION

3.1. Chemical Study of the Hybrid Epoxy Composites.

The completeness of the curing process was proved by the disappearance of the characteristic adsorption bands of uncured epoxy resin (ENC) at 970, 912, and 870 cm^{-1} in the ATR-FTIR spectra of all cured epoxy systems (Figure S2). Furthermore, an increase of adsorption bands at 1100, 950, and 800 cm^{-1} was observed in the ATR-FTIR spectra of the samples prepared using AP (i.e., for E12AP, E6AP_6HAURAPP, and E12AP_12HAURAPP samples).[18] These features might suggest the formation of a hybrid epoxy phase containing silicon (i.e., of an organic−inorganic structure), as already proved in previous papers.[1,18] In addition, the increase of the FTIR signals at about 3400, 2920, and 2870 cm^{-1}, related to the N−H asymmetric deformation vibration,[21] confirms the presence of APP in E6AP_6HAURAPP and E12AP_12HAURAPP samples.

The presence of HA in E6AP_6HAURAPP, E12AP_12HAURAPP, ENC+HA, and HA+IDA samples can be supported by the appearance of the FTIR bands around 3300 cm^{-1}, which are attributed to the O−H stretching of the oxygen-containing functional groups (i.e., carboxyl, phenol, and alcohol),[1,13,22,23] and at 1580 cm^{-1}, related to the C═O bonds, and ketone and quinone moieties (Figures S2−S4). Moreover, these bands are more intense in the FTIR spectra of the samples containing UR, proving its presence within the matrix. Furthermore, physical mixtures of HA with ENC or IDA, which underwent the same cure and post-cure treatments as the other hybrid epoxy composites, did not evidence any significant change in the related FTIR spectra, suggesting that no reaction occurred between HA and ENC or IDA during the curing process (Figures S3 and S4).

https://doi.org/10.1021/acsapm.1c01240
ACS Appl. Polym. Mater. 2021, 3, 5969−5981

3.2. Thermal Analysis. Figure 2a,c shows the thermogravimetric curves of E, E12AP, E12AP_12HAURAPP, and E6AP_6HAURAPP samples recorded in N_2 and air atmosphere, respectively. In N_2 atmosphere, a first weight loss occurs at about 280 °C; this finding is ascribed to the production of some volatile products, specifically acrolein, acetone, and allyl alcohol, as already reported in the literature.[24,25] The main decomposition step of the cross-linked resin (beyond 340 °C) occurs through the release of high-molecular-weight products along with more complex phenolic compounds.[25] Conversely, no weight changes were observed between 400 and 600 °C, due to the production of a very stable aromatic char (Figure 2a,b).

In air (Figure 2c,d), two main degradation steps around 350 and 500 °C are evident, in agreement with the degradation pathways of an aliphatic epoxy resin.[25,26]

Besides, the incorporation of AP leads to the appearance of a second degradation step at around 400 °C in N_2 atmosphere and to a shift of the oxidative degradation phenomena toward higher temperatures in air atmosphere, possibly due to the hybrid epoxy network that provides a higher thermal stability to the epoxy matrix (Figure 2).[27,28]

The presence of any of the employed additives improves the overall thermal behavior of the samples, providing higher residues with respect to the neat resin E, which, conversely, decomposes completely (Table S3).

HA positively affects the thermal behavior of the epoxy systems, because of the generation of a stable aliphatic char under inert atmosphere at high temperatures, resulting in an increase of the residue as compared to E.[14,29] In fact, the addition of HA (i.e., EAP_HA and E_HA samples, respectively, Table S3) leads to a faster decomposition of the resin chains, due to the acidic features of HA, which favor the char formation during the pyrolysis process.[14,21] Notably, the aromatic nature of HA allows the production of a more stable char during the degradation of E in air atmosphere, preventing the full oxidation of the resin with the formation of low-molecular-weight molecules[14,26,30] (Table S3, Section 3.1). In addition, the combined presence of HA and each of the other additives within the resin further improves the thermal behavior: in fact, the charring phenomenon is further supported by the presence of AP-modified DGEBA moieties containing siloxane groups that show a weak acidic character.

In air, the presence of AP in the epoxy matrix leads to the formation of a silicon-rich char, which acts as a thermal shield and protective barrier, preventing oxygen diffusion, hence further enhancing the thermo-oxidative stability (Table S3).

Besides, an abundant char formation is further expected by the degradation of the samples containing APP, whose decomposition produces acid phosphorus species and non-flammable volatiles (i.e., P-species and N_2), promoting a strong dehydration of the polymer matrix. Then, the phosphoric acids obtained by APP decomposition might react with the amino groups of the AP-modified DGEBA moieties, generating P−N−O substructures on the char surface, which improve its intumescence, as well as its efficacy as oxygen barrier during combustion.[30,31] Also, the decomposition of UR produces NH_3 that can be exothermically oxidized to N_2, hence leading to a dilution of the gas phase and a delay of the ignition time.[16,30,32]

Therefore, the E12AP_12HAURAPP sample may combine the beneficial effects of HA, APP, and AP on the overall thermal stability with those provided by UR, which is capable of diluting the flammable volatiles in the gas phase and generating an intumescent char with excellent fire retardant properties.[31] This hypothesis is confirmed by experimental data showing that the E12AP_12HAURAPP sample has the best thermal performance, combining one of the highest residues with self-extinguishing properties.

Table S4 shows the glass transition temperatures (T_g) measured by DSC analysis for pristine epoxy resin and all of the epoxy composites. No residual exothermic peak was observed during the first heating cycle, demonstrating the completeness of the curing reaction in the adopted conditions.

It is worth pointing out that the presence of the silane coupling agent in the polymer matrix (E12AP sample) does not affect the T_g of the composite; hence, it does not influence the epoxy chain's mobility (Table S4).[16,18]

The incorporation of HA into the epoxy resin (E_12HA sample) promoted an increase of T_g (by 17%) with respect to the value recorded for E (Table S4). This finding may be explained considering the formation of H-bonds between the oxygen-containing functional moieties of HA (see Section 3.1) and the hydroxyl groups formed during the cross-linking process.[1,30,33,34] In addition, the polar moieties of HA can interact with the epoxy groups of DGEBA chains to assure compatibility, hence contributing to enhance the stiffness of the epoxy network.[34] The effect of HA on the epoxy matrix (E_12HA sample) is also supported by the DMA results (Table S5) showing an increase of tan δ by 25%, as compared to the cured neat epoxy resin. Table S5 and Figure 3 show that

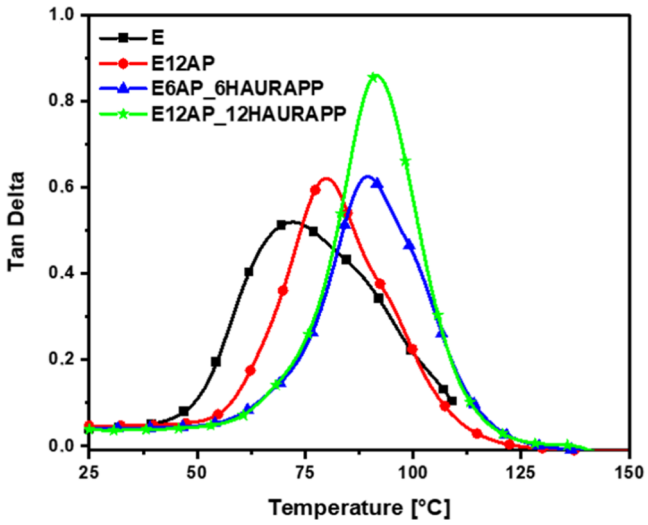

Figure 3. Mechanical damping factor (tan δ) of pristine resin and epoxy composites collected as a function of temperature.

the incorporation of HA into the epoxy resin accounts for higher tan δ values compared to those not containing the biowaste. Therefore, the mobility of the IDA aliphatic hardener does not hinder the network curing, and the use of HA leads to higher-cross-linked materials.[35]

Besides, UR is a diamide able to form a strong intersegmental hydrogen-bonded network with epoxy resin systems.[36,37] It is known that APP can interact with melamine polyphosphate flame retardants, which are employed for the manufacturing of glass-reinforced epoxy composites.[12] Therefore, considering the DSC results obtained for E_URAPP, it can be noted that APP and UR can strongly impact the epoxy chain's mobility, increasing the glass transition temperature from 75 °C, for pristine resin, to 89 °C for E_URAPP (Table

https://doi.org/10.1021/acsapm.1c01240
ACS Appl. Polym. Mater. 2021, 3, 5969−5981

S4). Finally, the combined use of APP, UR, and HA (E12AP_12HAURAPP, E6AP_6HAURAPP, and E_12HAURAPP samples) may favor the occurrence of hydrogen bond interactions between the oxygen-containing functional groups of HA (see Section 3.1) and nitrogen-based additives (i.e., UR and APP), resulting in an increase of T_g (up to about 17%) with respect to E and E12AP samples (Table S4 and Figure 4).[1,12,36]

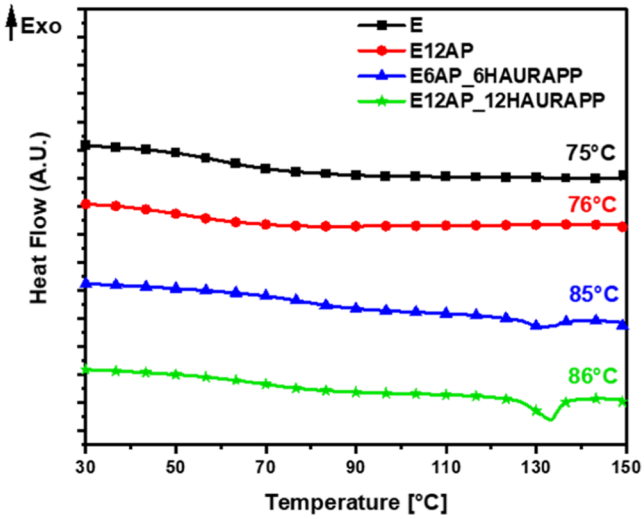

Figure 4. T_g of pristine resin and hybrid epoxy systems.

The DMA results shown in Table S5 additionally highlight that the presence of hybrid epoxy moieties in AP-modified DGEBA promotes the above-mentioned interactions between HA und UR. E12AP_12HAUR shows 56% increase of E' compared to the value shown by neat resin, though its tan δ appears to be lower than that of E12AP_12HAURAPP, which contains APP (Table S5).[12,30,35] These findings can be interpreted on the basis of the interactions occurring between HA und UR in the presence of AP (i.e., the E12AP_12HAUR sample), which lead to a material with a strong capability to store energy in its elastic portion but showing an increased free volume and thus a lower cross-linking density.[35] The incorporation of APP (i.e., the E12AP_12HAURAPP sample) causes the establishment of H-bonds with UR and helps in achieving a good compromise between tan δ and the storage modulus, thus yielding a highly cross-linked epoxy system with enhanced stiffness (Table S5 and Figure 5).[12,37,38]

3.3. Fire Behavior of the Hybrid Epoxy Composites.

Vertical flame spread tests were carried out on all of the epoxy composites to assess their flammability. E12AP_12HAURAPP was found to be self-extinguishing and V-0 rated (Figure S5). On the contrary, all of the other investigated samples were not classifiable (Table 2), though the formation of an abundant and coherent char was observed in the composites containing both AP and HA. The highest production of char occurred in the E12AP_12HAAPP sample, where the acid phosphorus compounds released by APP during its decomposition contributed to dehydration of the epoxy resin, through a synergistic effect with hybrid chains and HA additives. In addition, the presence of both AP and HA in the epoxy matrix prevented dripping (Table 2), due to the increase of the melt viscosity of the burning system.[39] Considering the afterflame times (t_1 and t_2 values, Table 2) of E_URAPP, E12AP_UR-

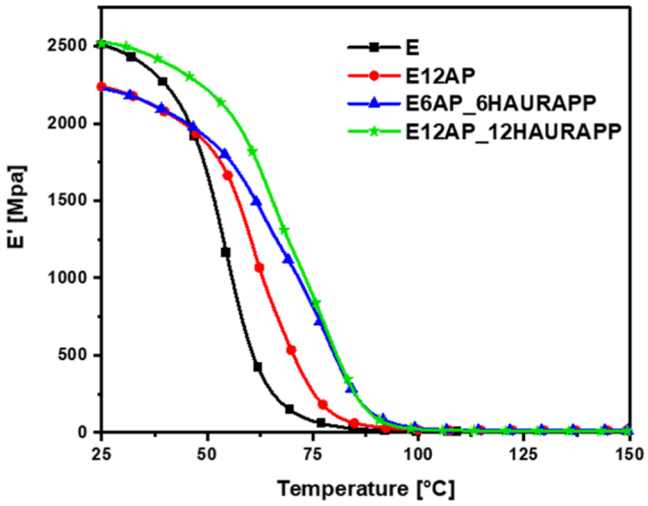

Figure 5. Storage moduli (E') of pristine resin and epoxy composites collected as a function of temperature.

APP, and E12AP_12HAURAPP samples, the incorporation of HA into the epoxy resin was crucial to obtain V-0 rating; the sample containing AP, HA (6 wt %), UR, and APP burned partially, producing a very coherent char (Figure S5). This also suggests a combined condensed-phase action exerted by HA and the hybrid epoxy moieties, which strongly affects the charring process from the early combustion stages. For E_URAPP and E12AP_URAPP samples, a decrease in flame inhibition after the first application of flame was observed (Table 2). However, E12AP_URAPP showed lower t_1 values, which may be due to the high char-forming character of the AP-modified epoxy network, able to generate a silicon-rich char acting as a thermal shield and oxygen barrier for the underlying polymer matrix.[37] Conversely, the use of APP and UR blowing agents was fundamental to positively influence the t_1 extinguishing time (sample E_URAPP, Table 2), especially when the epoxy resin did not undergo sol−gel modification.[30,32,40] This finding was ascribed to the decomposition of APP and UR, since the former acts in the gas phase, forming phosphorus species, whereas the latter produces nitrogen-based volatiles, leading to the dilution of flammable volatiles and increasing the extinguishing time t_1 with respect to the other unmodified formulations.

During the CC tests, the decreases of pHRR (ranging from 39 to 52%) and THR (up to 23%) were more pronounced for the composites containing HA, UR, and APP (Figures 6 and S6, Table 3), though the presence of AP alone (the E12AP sample) significantly lowered the aforementioned parameters. However, an increase of the amounts of AP, HA, UR, and APP delayed the time to pHRR (Table 3). This effect can mainly be ascribed to the decomposition of APP and UR, as clearly reported in the literature.[27,33,41,42]

Cone calorimetry results (Table 3 and Figure S6) confirm that the highest impact on the flame retardance of the composites is due to the acidic character of the hybrid epoxy chains, exerting a strong condensed-phase activity through dehydration of the network and leading to a remarkable reduction of the pHRR, mass loss rate (MLR), and FPI, but also to an increase of the residual mass and TTP. However, as previously mentioned for the vertical flame spread tests, the addition of HA in combination with AP, UR, and APP was crucial to achieve self-extinction. Figure 6 shows a noticeable

https://doi.org/10.1021/acsapm.1c01240
ACS Appl. Polym. Mater. 2021, 3, 5969−5981

Table 2. Results of Flame Spread Tests in Vertical Configuration[a]

sample	t_1 in s					t_2 in s					UL 94/dripping
E											not classifiable (NC)/yes
E_12HA											NC/no
E_UR											NC/no
E_APP											NC/no
E_URAPP	8	7	6	7	8						NC/no
E_12HAUR											NC/no
E_12HAAPP											NC/no
E_12HAURAPP											NC/no
E12AP											NC/no
E12AP_12HA											NC/no
E12AP_UR											NC/no
E12AP_APP											NC/no
E12AP_URAPP	3	3	4	5	3						NC/no
E12AP_12HAUR											NC/no
E12AP_12HAAPP											NC/no
E6AP_6HAURAPP											NC/no
E12AP_12HAURAPP	0	0	0	0	0	0	0	0	0	0	V-0/no

[a] t_1 and t_2 = Duration of flaming after the first and second flame application. The test was carried out 5 times for all of the samples.

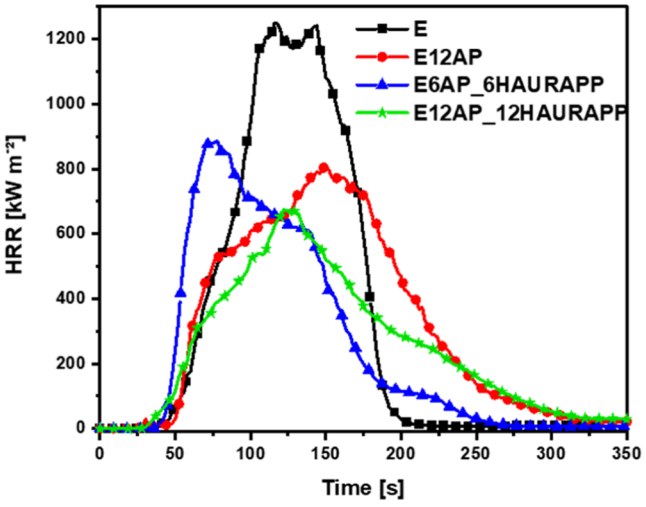

Figure 6. Heat release rate (HRR) versus time for E, E12AP, E6AP_6HAURAPP, and E12AP_12HAURAPP samples.

broadening of the HRR curve for E12AP_12HAURAPP, where the phosphorus species stop the hydrocarbon oxidation reactions and slow down the branching and chain reactions occurring in the gas phase, thus reducing the heat production.[33] An additional increase of the residue was observed in E12AP_12HAURAPP and E6AP_6HAURAPP samples (Table 3), where the additives favor the formation of a coherent, swollen, and intumescent char (Figure 7). This can be ascribed to the release of the nitrogen species and dehydration of the matrix by the acidic hybrid epoxy moieties, HA, and phosphorus species formed during combustion.[32,43] The strong increase in CO/CO_2 ratio observed for E12AP_12HAURAPP and E6AP_6HAURAPP (Table 3 and Figure S6) may be due to the APP that releases phosphorus species in the gas phase, leading to an incomplete combustion and consequently to the formation of CO. These phosphorus species interrupt and slow down the branching and chain reactions of the hydrocarbon oxidation reactions in the gas phase, thus reducing the heat production and leading to flame inhibition.[33,41]

To better elucidate the fire behavior of the epoxy samples, time to flashover (TTF) and flame propagation index (FPI) were calculated (Table 3).[43,44] The first parameter represents the time available to escape a fire in a confined space[44−46] (see Section S4), while the second one depends on the flammability (i.e., front flame movement). E12AP_12HAURAPP and E6AP_6HAURAPP samples showed significantly increased TTF and, therefore, were characterized by lower FPI, smoke production rate (SPR), and total smoke release (TSR) with respect to the pristine resin (Table 3 and Figure S6). The decomposition of HA, UR, and APP generates greener compounds replacing several aromatic structures (e.g., benzene, naphthalene, anthracene, among a few to mention), which are normally produced during the last steps of the carbonization and gas-phase combustion processes of a DGEBA resin.[47−51] These phenyl-based compounds are the main components of smoke during the degradation of an epoxy resin.[25,48,52]

Table 3. Results from Cone Calorimetry Tests for the Investigated Samples[a]

sample	TTI [s]	pHRR [kW/m²]	TTP [s]	THR [MJ/m²]	TSR [m²/m²]	RM [%]	FPI	TTF [min]	CO/CO_2
E	28	1471	125	111	3755	3	52		0.29
E12AP	25	856	160	111	3493	7	34	0.5	0.26
E6AP_6HAURAPP	34	902	78	86	2913	9	26	1.6	0.44
E12AP_12HAURAPP	28	704	128	88	3145	11	25	1.8	0.41

[a] TTI = time to ignition, pHRR = peak of the heat release rate, TTP = time to peak, THR = total heat release, TSR = total smoke release, RM = residual mass, FPI = flame propagation index, TTF = time to flashover, FRI = flame retardancy index. FRI is not reported for EPO, because this sample represents the neat polymer.

https://doi.org/10.1021/acsapm.1c01240
ACS Appl. Polym. Mater. 2021, 3, 5969−5981

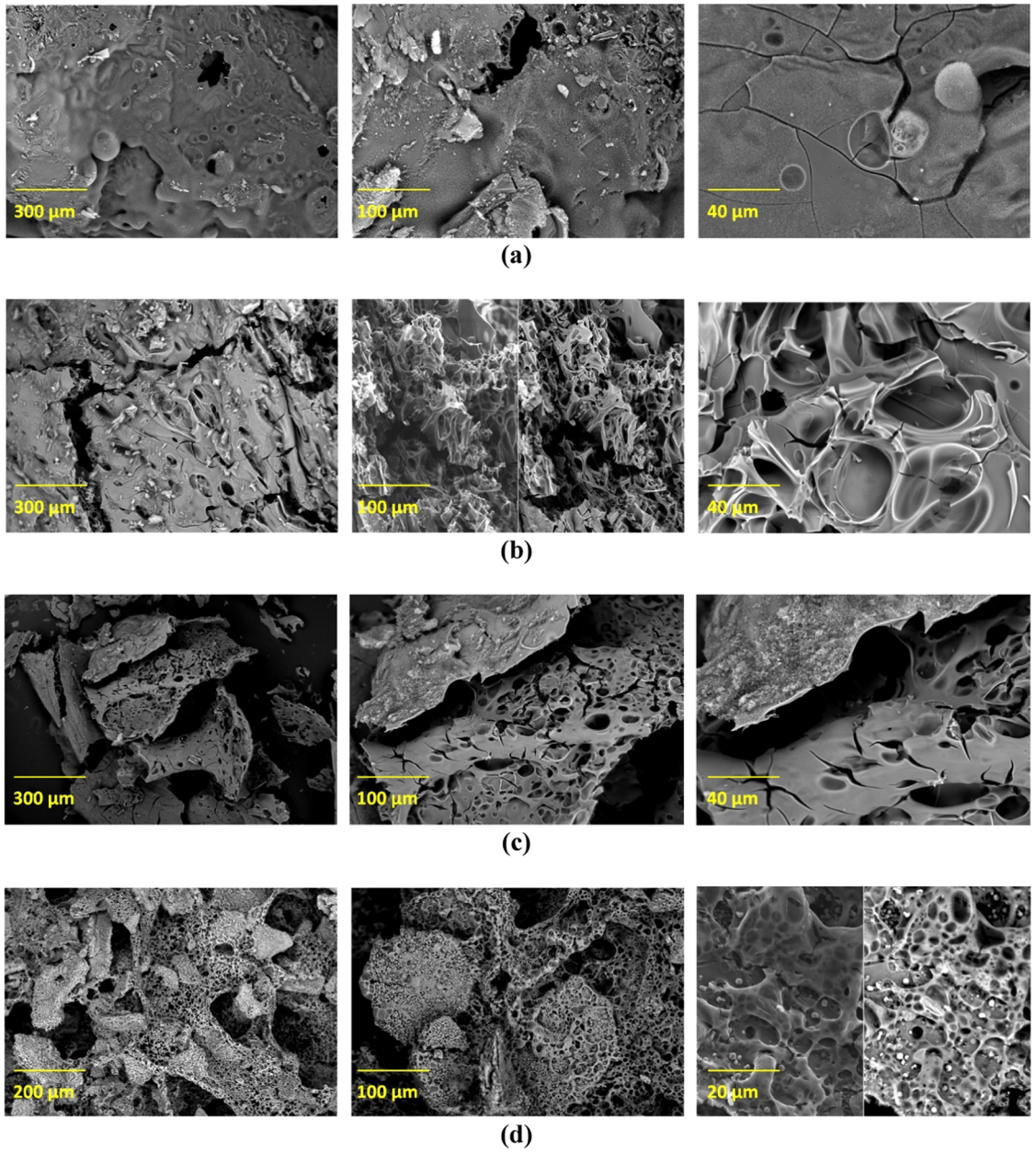

Figure 7. SEM images of the residual char obtained after the CC test of E (a), E12AP (b), E6AP_6HAURAPP (c), and E12AP_12HAURAPP (d) samples.

3.4. Thermal Decomposition and Flame Retardant Mechanism Studies. DIP-MS analysis was performed on E, E12AP, E12AP_12HAURAPP, and E6AP_6HAURAPP to further elucidate the decomposition mechanism and the influence of each additive on the gases evolved. As already reported for similar systems, the decomposition pathway for epoxy resins in inert atmosphere and at high temperature mainly leads to the formation of bisphenol A, 4,4′-(cyclopropane-1,1-diyl)diphenol, 4-isopropylphenol, 4-isopropenylphenol, phenol, benzene, naphthalene, toluene, 2-methylpent-2-en-1-ol, 3-hydroxy-2-methylpentanal, *o*-cresol, 2-ethylphenol, and 2-allyl-4-methylphenol, along with low amounts of aromatic products, which are recognized as the most abundant products[25,53,54] (Figure S7, Table S6).

Figure 8 shows the total ion thermograms for E, E12AP, E12AP_12HAURAPP, and E6AP_6HAURAPP samples obtained through DIP-MS analysis, which additionally confirmed the formation of many decomposition products. Besides, Figure S7 confirms that E, E12AP, E12AP_12HAURAPP, and E6AP_6HAURAPP samples release approximately the same amount of decomposed volatile species (namely, bisphenol A, 4,4′-(cyclopropane-1,1-diyl)diphenol, 4-isopropylphenol, 4-isopropenylphenol, and phenol) by increasing the temperature up to 450 °C. In particular, DIP-MS results (Figure S8) highlight the production of more species for E12AP_12HAURAPP and E6AP_6HAURAPP samples between 200 and 450 °C, as APP decomposes and phosphorus species are released (Table S7).[55] The presence of these phosphorus compounds was already observed for APP, although in a different polymer matrix.[55,56] In air, $PO^{\bullet}$ radicals can act in the gas phase and consume active $H^{\bullet}$ and $OH^{\bullet}$ species in the flame by recombining with them and favoring flame inhibition.[57,58] DIP-MS results and the detection of phosphorus radicals agree with an increased value of CO/CO_2

https://doi.org/10.1021/acsapm.1c01240
ACS Appl. Polym. Mater. 2021, 3, 5969−5981

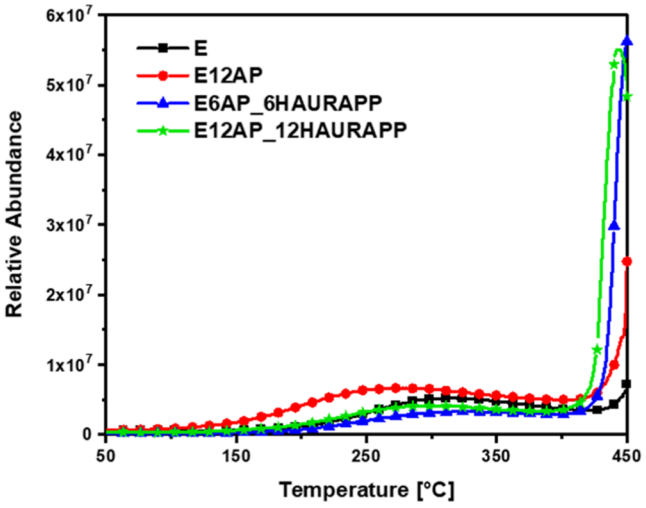

Figure 8. DIP-MS total ion thermograms of E, E12AP, E12AP_12HAURAPP, and E6AP_6HAURAPP samples.

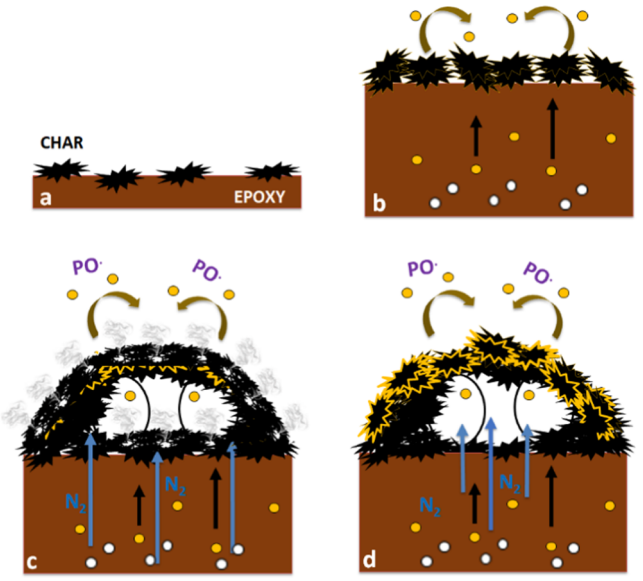

Figure 9. Proposed mechanism of E-AP/APP-UR-HA in oxygen (O_2) atmosphere. (a) E, (b) E12AP, (c) E6AP_6HAURAPP, and (d) E12AP_12HAURAPP. Black arrows show the direction of rising bubbles (white balls) from the hot polymer matrix (borrow region). Yellow circles indicate the sol−gel hybrid epoxy moieties in the network. In particular, the yellow border line around the black carbonaceous char indicates the presence of a silicon-rich char (thermal shield and oxygen barrier) on the surface of the burning sample.

ratios for E12AP_12HAURAPP and E6AP_6HAURAPP compared to E and E12AP samples, as assessed by cone calorimetry tests (see Section 3.3). Figure S8 displays the thermograms of each species formed from the decomposition of APP.

Scheme S1 shows a possible mode of reaction between APP and E during degradation in air. In the presence of APP, the active radicals $O^{\bullet}$ in the flame zone are neutralized and turned into a notable amount of volatile species such as $PO^{\bullet}$, $PO_2^{\bullet}$, and $HOPO_2^{\bullet}$ (flame inhibitors).[30,41]

The E12AP_12HAURAPP sample shows a larger amount of $PO^{\bullet}$ radicals released during the combustion compared to E6AP_6HAURAPP, confirming that the involved gas-phase mechanism accounts for the excellent performance in the UL 94 test of this sample. A higher production of flame inhibitors from the early stages of epoxy degradation and the formation of a continuous swollen multicellular char may further justify the self-extinguishing behavior of E12AP_12HAURAPP compared to the E6AP_6HAURAPP sample. Also, DIP-MS analysis of these samples showed the release of nitrogen species at around 250 °C without any significant change in the epoxy resin degradation. These nitrogen-based compounds are produced by the decomposition of UR and APP, as reported in the literature for other composites.[48] In particular, UR mainly affects the flame retardance of hybrid epoxy composites through the activity of N_2 that dilutes the combustible gases, hence playing a physical role in the general mode of reaction between APP and E.[27,32] Therefore, UR influences the flammability of resin (Section 3.3, Tables 2 and 3) without any chemical interaction with the main degradation products of the epoxy network. For these reasons, UR does not appear in Scheme S1.

Based on elemental (Table S8) and SEM analyses of residual char (Figure 7), a combined effect of HA, UR, APP, and AP acting in both condensed and gas phases is proposed (Figure 9). It is well known that epoxy resins are well-established charring polymers and undergo carbonization processes during combustion.[59] As previously observed in thermogravimetric analysis (Section 3.2), HA may boost the dehydration kinetics because of its acidic character, affecting decomposition temperatures and the final residue under N_2 atmosphere. A similar condensed-phase activity occurs due to the presence of the hybrid domains, which address the pyrolysis toward the formation of a silicon-rich char on the material surface.[60] The latter works as a thermal shield toward the spread of gaseous species supplied from the decomposing polymer bulk, and of oxygen.[52] The detection of silicon elements in addition to C, H, and N, which are dominating in the char of the pristine epoxy sample (E sample, Figure 9a), proves the production of a silicon-rich char in the case of E12AP (Table S8, Figure 9b). As regards SEM analysis (Figure 7a,b), it is evident that the char morphology of E12AP is more compact and coherent compared to that of E, in which fractures and holes are present. These findings justify the improved fire behavior of E12AP compared to E observed in the forced-combustion tests (Table 3),[18] as the hybrid epoxy network is responsible for a reduction of pHRR as high as 42%.

The scientific literature well reports that UR and APP degrade at around 250 °C, releasing NH_3 that undergoes exothermic decomposition, forming N_2.[58,61] Besides, the degradation of APP produces acid phosphorus compounds during combustion, which, together with HA, are responsible for the generation of an intumescent and abundant char along the dehydration.[32,40] In addition, NH_3 may also react with polyphosphoric acid to produce P−N−O substructures, hence providing insulating properties to the intumescent char.[30,31] Further, the combined use of HA, UR, and APP (the E6AP_6HAURAPP sample) is responsible for the formation of an intumescent char characterized by the presence of P−N−O−Si−O−P polymeric substructures on the surface (Figure 9c).[31,43] The latter are obtained through condensation between silanol groups (i.e., Si−O−Si) of the hybrid epoxy network and P−N−O substructures. This char behaves as a thermal shield and oxygen barrier at the boundary layer,[40,52,53] leading to a high retention of P for E6AP_6HAURAPP (Table

https://doi.org/10.1021/acsapm.1c01240
ACS Appl. Polym. Mater. 2021, 3, 5969−5981

S8) and a strong delay in the ignition time and time to flashover (Table 3). However, the synergism of these effects was not enough to achieve self-extinction (Table 2). In this regard, the E12AP_12HAURAPP sample (Figure 9d), prepared with a higher amount of additives, showed a swollen multicellular intumescent char and higher retention of P as compared to E6AP_6HAURAPP (Figure 7c,d, Table S8). Therefore, it is reasonable to hypothesize that this swollen multicellular intumescent char contains a higher number of P−N−O−Si−O−P polymeric substructures on the surface.[30] SEM analysis supports this hypothesis, since the char morphology of E6AP_6HAURAPP appears intermediate between those produced by E12AP and those produced by E12AP_12HAURAPP, because the multicellular structures are not uniformly formed yet (Figures 7 and 9).

Hence, E12AP_12HAURAPP may exert a strong condensed-phase mechanism, resulting in excellent performances in UL 94 (V-0 class) and CC tests (52% of pHRR reduction, Table 3), despite the use of an aliphatic amine (IDA) as the hardener.

The interaction of hybrid moieties, phosphorus flame retardants, and nitrogen additives to form a stable char and resulting in an improved fire performance is well known for other polymeric systems, though, based on the best knowledge of the authors, this is the first time that a biowaste (i.e., HA) becomes a crucial component in the flame retardance of an epoxy-based system.[14,31,62,63]

3.5. Mechanical Behavior. The tensile properties of E, E12AP, E12AP_12HAURAPP, and E6AP_6HAURAPP samples were measured according to the ASTM D638 standard (Table 4). It is well known that the formation of silicon-containing hybrid moieties can be considered an effective method for increasing the toughness of epoxies.[64] The presence of hybrid epoxy chains in the polymer matrix slows down the kinetics of the energy dissipation mechanisms, as for example the crack growth occurring from filler debonding. Thus, the incorporation of a hybrid epoxy network into neat epoxies promotes an increase of fracture toughness.[64] Therefore, the E12AP sample, which was synthesized by following the first step of a sol−gel method already exploited by the authors in several similar systems,[16,18,30,48] is characterized by uniformly distributed hybrid moieties that increase its fracture strength "σ_B" and elongation break "ε_B" compared to the E sample (Table 4). The incorporation of HA, UR, and APP into the hybrid epoxy composites (E6AP_6HAURAPP and E12AP_12HAURAPP samples) does not seem to significantly affect the overall mechanical behavior of the cured epoxy resin (Table 4).

Table 4. Tensile Test Results of Pure Epoxy Resin (E) and Epoxy Composites for Comparison

sample	E_t [MPa]	σ_B [MPa]	ε_B [%]
E	1900 ± 157	38.3 ± 17.7	3.7 ± 2.3
E12AP	1760 ± 33	60.4 ± 2.5	10.0 ± 3.2
E6AP_6HAURAPP	1810 ± 156	36.3 ± 15.1	3.3 ± 2.1
E12AP_12HAURAPP	2030 ± 68	38.6 ± 4.1	3.5 ± 0.6

The literature indicates that self-extinction can be achieved for DGEBA-based systems in a P-containing bio-resin, prepared with itaconic acid (IA) and 9,10-dihydro-9-oxa-10-phosphaphenanthrene 10-oxide (DOPO), which was used as a bio-based flame retardant in the DGEBA system.[65] This modification allowed the formation of a phosphorus-containing bio-epoxy resin system, where the synthetic resin completely changes its structure and can be cured using methyl hexahydrophthalic anhydride. Even though this methodology was very effective in terms of fire behavior, it required a high concentration of phosphorus (∼4 wt %) to achieve V0 class in UL 94 vertical flame spread tests.[66] Conversely, the addition of HA in combination with AP, UR, and APP (i.e., E12AP_12HAURAPP sample) helps in achieving self-extinction with 1.1 wt % of phosphorus only. Besides, it is well known from the literature that phenethyl-bridged DOPO derivatives in combination with organo-modified aluminum hydroxide (OATH) can provide DGEBA-based epoxy systems with flame retardant features.[67−69] In particular, 10 wt % phenethyl-bridged DOPO derivative and 60 wt % OATH were incorporated into DGEBA cured with 2-ethyl-4-methylimidazole. The resulting system achieved UL 94 V0 rating thanks to the "sink effect" provided by OATH, which delayed the TTI of the composite.[70] Despite the achievement of self-extinction features, the high OATH loading showed a detrimental effect on the mechanical performances, which exhibited a significant loss of toughness.[69] On the contrary, our proposed strategy does not negatively affect the mechanical behavior of the epoxy system, as clearly shown by the values of stiffness and elongation at break presented in Table 4 (see E12AP_12HAURAPP sample). In conclusion, E12AP_12HAURAPP shows mechanical performances comparable to the neat epoxy matrix, as well as self-extinguishing capability, which make this formulation very promising for possible future industrial applications.

4. CONCLUSIONS

In this work, humic acid (HA) as a biowaste flame retardant (i.e., active in condensed phase), urea (UR) as nitrogen source, and ammonium polyphosphate (APP) as a phosphorus-based intumescent flame retardant were added to a silicon-modified epoxy resin to improve its fire performances. Thermal and microscopy analysis revealed that the incorporation of HA strongly promotes the thermal stability of the epoxy system by boosting the char-forming process; therefore, HA is the contributing factor to the strong condensed-phase activity due to its chemical structure. Furthermore, the presence of humic acid in the epoxy system prevented melt dripping during the vertical flame spread tests, and the formulation containing HA (6 wt %), UR (4 wt %), and APP (6 wt %) allowed to achieve self-extinguishing capability with an unprecedented very low phosphorus concentration (∼1 wt %). Forced-combustion tests showed that the addition of HA, UR, and APP to the hybrid epoxy system promoted a strong reduction of pHRR values up to 52%, together with an increase of the time to flashover and residue. The excellent flame retardant results were ascribed to the formation of an N−P−O−Si chain containing intumescent char, which acts as a thermal shield and oxygen barrier, and a gas-phase activity of APP linked to the flame inhibition mechanism.

In conclusion, we demonstrated that a biowaste flame retardant such as humic acid can be well dispersed into a silicon-modified DGEBA resin, since silicon-containing hybrid epoxy moieties help in achieving a uniform distribution of the filler. In addition, a simple combination of inexpensive additives (HA, UR, and APP) with a low amount of phosphorus accounts for the excellent flame retardant features of epoxy resins even cured with an aliphatic hardener, without

https://doi.org/10.1021/acsapm.1c01240
ACS Appl. Polym. Mater. 2021, 3, 5969−5981

any negative effect on the overall mechanical performances. This study may contribute to the setting up of effective methodologies to exploit the flame retardant features of HA toward the development of new green, effective composite materials. Finally, this strategy may inspire the design of more sustainable products, where the polymer matrix is also bio-based.

■ ASSOCIATED CONTENT

Supporting Information

The Supporting Information is available free of charge at https://pubs.acs.org/doi/10.1021/acsapm.1c01240.

Preparation of silica-epoxy composite; composition and codes of the investigated epoxy samples; chemical characterization of the silica-epoxy composites; ATR-FTIR spectra for all the prepared formulations; thermal analysis; results from thermogravimetric analysis of all samples in air and N_2; T_g data from DSC thermograms (second heating cycle) of all investigated samples; DMA results for of all investigated samples; fire behavior of the hybrid epoxy composites; calculation of flame propagation index and time to flashover from cone calorimeter measurements; residues after UL 94 VB tests; CO yield (%), CO_2 yield (%), mass loss rate, smoke production rate, total heat release, total smoke release curves of samples measured by cone calorimeter; major decomposition products of pristine epoxy with cycloaliphatic hardener under N_2 atmosphere; DIP-MS analysis of samples measured by cone calorimeter; thermal decomposition and flame retardant mechanism studies; major decomposition products of ammonium polyphosphate flame retardant; proposed mechanism of E-APP reactions in oxygen (O_2) atmosphere; and energy-dispersive X-ray analysis elemental composition of the char residue of samples measured by cone calorimeter (PDF)

■ AUTHOR INFORMATION

Corresponding Authors

Giuseppina Luciani − *Department of Chemical Materials and Industrial Production Engineering (DICMaPI), University of Naples Federico II, Fuorigrotta 80125, Italy;* orcid.org/0000-0002-1169-0137; Email: luciani@unina.it

Aurelio Bifulco − *Department of Chemical Materials and Industrial Production Engineering (DICMaPI), University of Naples Federico II, Fuorigrotta 80125, Italy;* orcid.org/0000-0002-4214-5385; Email: aurelio.bifulco@unina.it

Authors

Virginia Venezia − *Department of Chemical Materials and Industrial Production Engineering (DICMaPI), University of Naples Federico II, Fuorigrotta 80125, Italy;* orcid.org/0000-0002-6368-2681

Samuele Matta − *Department of Applied Science and Technology, Polytechnic University of Turin, Alessandria 15121, Italy*

Sandro Lehner − *Laboratory for Advanced Fibers, Empa Swiss Federal Laboratories for Materials Science and Technology, St. Gallen 9014, Switzerland*

Giuseppe Vitiello − *Department of Chemical Materials and Industrial Production Engineering (DICMaPI), University of Naples Federico II, Fuorigrotta 80125, Italy;* orcid.org/0000-0003-3389-6942

Aniello Costantini − *Department of Chemical Materials and Industrial Production Engineering (DICMaPI), University of Naples Federico II, Fuorigrotta 80125, Italy;* orcid.org/0000-0002-3053-6995

Sabyasachi Gaan − *Laboratory for Advanced Fibers, Empa Swiss Federal Laboratories for Materials Science and Technology, St. Gallen 9014, Switzerland;* orcid.org/0000-0001-9891-5249

Giulio Malucelli − *Department of Applied Science and Technology, Polytechnic University of Turin, Alessandria 15121, Italy;* orcid.org/0000-0002-0459-7698

Francesco Branda − *Department of Chemical Materials and Industrial Production Engineering (DICMaPI), University of Naples Federico II, Fuorigrotta 80125, Italy;* orcid.org/0000-0003-3216-9081

Complete contact information is available at: https://pubs.acs.org/10.1021/acsapm.1c01240

Author Contributions

The manuscript was written through the contributions of all authors, and all authors have given approval to the final version of the manuscript.

Funding

Any funds used to support the research of the manuscript.

Notes

The authors declare no competing financial interest.

■ REFERENCES

(1) Pota, G.; Venezia, V.; Vitiello, G.; Di Donato, P.; Mollo, V.; Costantini, A.; Avossa, J.; Nuzzo, A.; Piccolo, A.; Silvestri, B.; et al. Tuning Functional Behavior of Humic Acids through Interactions with Stöber Silica Nanoparticles. *Polymers* **2020**, *12*, 982.

(2) Venezia, V.; Pota, G.; Silvestri, B.; Vitiello, G.; Di Donato, P.; Landi, G.; Mollo, V.; Verrillo, M.; Cangemi, S.; Piccolo, A.; et al. A study on structural evolution of hybrid humic Acids-SiO2 nanostructures in pure water: Effects on physico-chemical and functional properties. *Chemosphere* **2022**, No. 131985.

(3) Kümmerer, K.; Clark, J. H.; Zuin, V. G. Rethinking chemistry for a circular economy. *Science* **2020**, *367*, 369−370.

(4) Bańkowski, K.; Ferdinandusse, M.; Hauptmeier, S.; Jacquinot, P.; Valenta, V. The macroeconomic impact of the Next Generation EU instrument on the euro area. *ECB Occasional Paper* 2021, (2021/255). https://www.ecb.europa.eu/pub/pdf/scpops/ecb.op255~9391447a99.en.pdf (accessed Sept 22, 2021).

(5) Xu, C.; Nasrollahzadeh, M.; Selva, M.; Issaabadi, Z.; Luque, R. Waste-to-wealth: biowaste valorization into valuable bio (nano) materials. *Chem. Soc. Rev.* **2019**, *48*, 4791−4822.

(6) Ye, X.; Li, J.; Zhang, W.; Yang, R.; Li, J. Fabrication of eco-friendly and multifunctional sodium-containing polyhedral oligomeric silsesquioxane and its flame retardancy on epoxy resin. *Composites, Part B* **2020**, *191*, No. 107961.

(7) Qu, Z.; Wu, K.; Jiao, E.; Chen, W.; Hu, Z.; Xu, C.; Shi, J.; Wang, S.; Tan, Z. Surface functionalization of few-layer black phosphorene and its flame retardancy in epoxy resin. *Chem. Eng. J.* **2020**, *382*, 122991.

(8) Markwart, J. C.; Battig, A.; Zimmermann, L.; Wagner, M.; Fischer, J.; Schartel, B.; Wurm, F. R. Systematically controlled decomposition mechanism in phosphorus flame retardants by precise molecular architecture: P−O vs P−N. *ACS Appl. Polym. Mater.* **2019**, *1*, 1118−1128.

(9) Zhang, S.; Liu, X.; Jin, X.; Li, H.; Sun, J.; Gu, X. The novel application of chitosan: Effects of cross-linked chitosan on the fire

performance of thermoplastic polyurethane. *Carbohydr. Polym.* **2018**, *189*, 313−321.
(10) Glasing, J.; Champagne, P.; Cunningham, M. F. Graft modification of chitosan, cellulose and alginate using reversible deactivation radical polymerization (RDRP). *Curr. Opin. Green Sustainable Chem.* **2016**, *2*, 15−21.
(11) Ke, Y.; Yang, X.; Chen, Q.; Xue, J.; Song, Z.; Zhang, Y.; Madbouly, S. A.; Luo, Y.; Li, M.; Wang, Q.; et al. Recyclable and Fluorescent Epoxy Polymer Networks from Cardanol Via Solvent-Free Epoxy-Thiol Chemistry. *ACS Appl. Polym. Mater.* **2021**, *3*, 3082−3092.
(12) Matykiewicz, D.; Przybyszewski, B.; Stanik, R.; Czulak, A. Modification of glass reinforced epoxy composites by ammonium polyphosphate (APP) and melamine polyphosphate (PNA) during the resin powder molding process. *Composites, Part B* **2017**, *108*, 224−231.
(13) Lee, S.; Roh, Y.; Koh, D.-C. Oxidation and reduction of redox-sensitive elements in the presence of humic substances in subsurface environments: A review. *Chemosphere* **2019**, *220*, 86−97.
(14) Liu, G.; Shi, H.; Kundu, C. K.; Li, Z.; Li, X.; Zhang, Z. Preparation of novel biomass humate flame retardants and their flame retardancy in epoxy resin. *J. Appl. Polym. Sci.* **2020**, *137*, 49601.
(15) Liu, C.; Chen, T.; Yuan, C. H.; Song, C. F.; Chang, Y.; Chen, G. R.; Xu, Y. T.; Dai, L. Z. Modification of epoxy resin through the self-assembly of a surfactant-like multi-element flame retardant. *J. Mater. Chem. A* **2016**, *4*, 3462−3470.
(16) Bifulco, A.; Parida, D.; Salmeia, K. A.; Nazir, R.; Lehner, S.; Stämpfli, R.; Markus, H.; Malucelli, G.; Branda, F.; Gaan, S. Fire and mechanical properties of DGEBA-based epoxy resin cured with a cycloaliphatic hardener: Combined action of silica, melamine and DOPO-derivative. *Mater. Des.* **2020**, *193*, No. 108862.
(17) Pant, R. R.; Buckley, J. L.; Fulmer, P. A.; Wynne, J. H.; McCluskey, D. M.; Phillips, J. P. Hybrid siloxane epoxy coatings containing quaternary ammonium moieties. *J. Appl. Polym. Sci.* **2008**, *110*, 3080−3086.
(18) Bifulco, A.; Tescione, F.; Capasso, A.; Mazzei, P.; Piccolo, A.; Durante, M.; Lavorgna, M.; Malucelli, G.; Branda, F. Effects of post cure treatment in the glass transformation range on the structure and fire behavior of in situ generated silica/epoxy hybrids. *J. Sol-Gel Sci. Technol.* **2018**, *87*, 156−169.
(19) Matějka, L.; Dušek, K.; Pleštil, J.; Kříž, J.; Lednický, F. Formation and structure of the epoxy-silica hybrids. *Polymer* **1999**, *40*, 171−181.
(20) Branda, F.; Bifulco, A.; Jehnichen, D.; Parida, D.; Pauer, R.; Passaro, J.; Gaan, S.; Pospiech, D.; Durante, M. Structure and Bottom-up Formation Mechanism of Multisheet Silica-Based Nanoparticles Formed in an Epoxy Matrix through an In Situ Process. *Langmuir* **2021**, *37*, 8886−8893.
(21) Yang, S.-s.; Chen, Z.-b. The Study on Aging and Degradation Mechanism of Ammonium Polyphosphate in Artificial Accelerated Aging. *Procedia Eng.* **2018**, *211*, 906−910.
(22) Gao, Y.; Pang, S.-Y.; Jiang, J.; Ma, J.; Zhou, Y.; Li, J.; Wang, L.-H.; Lu, X.-T.; Yuan, L.-P. Transformation of flame retardant tetrabromobisphenol A by aqueous chlorine and the effect of humic acid. *Environ. Sci. Technol.* **2016**, *50*, 9608−9618.
(23) Mayans, B.; Pérez-Esteban, J.; Escolástico, C.; Eymar, E.; Masaguer, A. Evaluation of commercial humic substances and other organic amendments for the immobilization of copper through 13C CPMAS NMR, FT-IR, and DSC analyses. *Agronomy* **2019**, *9*, No. 762.
(24) Yan, H.; Lu, C.-x.; Jing, D.-q.; Hou, X.-l. Chemical degradation of amine-cured DGEBA epoxy resin in supercritical 1-propanol for recycling carbon fiber from composites. *Chin. J. Polym. Sci.* **2014**, *32*, 1550−1563.
(25) Grassie, N.; Guy, M. I.; Tennent, N. H. Degradation of epoxy polymers: Part 1—Products of thermal degradation of bisphenol-A diglycidyl ether. *Polym. Degrad. Stab.* **1985**, *12*, 65−91.
(26) Musto, P.; Ragosta, G.; Russo, P.; Mascia, L. Thermal-Oxidative degradation of epoxy and epoxy-Bismaleimide networks: kinetics and mechanism. *Macromol. Chem. Phys.* **2001**, *202*, 3445−3458.
(27) Bretterbauer, K.; Schwarzinger, C. Melamine derivatives-a review on synthesis and application. *Curr. Org. Synth.* **2012**, *9*, 342−356.
(28) Jiao, J.; Liu, P.; Wang, L.; Cai, Y. One-step synthesis of improved silica/epoxy nanocomposites with inorganic-organic hybrid network. *J. Polym. Res.* **2013**, *20*, No. 202.
(29) Liu, X.; Salmeia, K. A.; Rentsch, D.; Hao, J.; Gaan, S. Thermal decomposition and flammability of rigid PU foams containing some DOPO derivatives and other phosphorus compounds. *J. Anal. Appl. Pyrolysis* **2017**, *124*, 219−229.
(30) Bifulco, A.; Parida, D.; Salmeia, K.; Lehner, S.; Stämpfli, R.; Markus, H.; Malucelli, G.; Branda, F.; Gaan, S. Improving Flame Retardancy of in-situ Silica-Epoxy Nanocomposites cured with Aliphatic Hardener: Combined effect of DOPO-based flame-retardant and Melamine. *Composites, Part C* **2020**, *2*, No. 100022.
(31) Gaan, S.; Sun, G.; Hutches, K.; Engelhard, M. H. Effect of nitrogen additives on flame retardant action of tributyl phosphate: phosphorus−nitrogen synergism. *Polym. Degrad. Stab.* **2008**, *93*, 99−108.
(32) Bourbigot, S.; Duquesne, S. Fire retardant polymers: recent developments and opportunities. *J. Mater. Chem.* **2007**, *17*, 2283−2300.
(33) Salmeia, K. A.; Gooneie, A.; Simonetti, P.; Nazir, R.; Kaiser, J.-P.; Rippl, A.; Hirsch, C.; Lehner, S.; Rupper, P.; Hufenus, R.; et al. Comprehensive study on flame retardant polyesters from phosphorus additives. *Polym. Degrad. Stab.* **2018**, *155*, 22−34.
(34) Wang, F.; Pan, S.; Zhang, P.; Fan, H.; Chen, Y.; Yan, J. Synthesis and application of phosphorus-containing flame retardant plasticizer for polyvinyl chloride. *Fibers Polym.* **2018**, *19*, 1057−1063.
(35) Mattar, N.; de Anda, A. R.; Vahabi, H.; Renard, E.; Langlois, V. Resorcinol-Based Epoxy Resins Hardened with Limonene and Eugenol Derivatives: From the Synthesis of Renewable Diamines to the Mechanical Properties of Biobased Thermosets. *ACS Sustainable Chem. Eng.* **2020**, *8*, 13064−13075.
(36) Fang, J.; Zuo, R.; He, P.; Quan, Y.; Chen, Q. The effect of urea bond on structure and properties of toughened epoxy resins. *J. Appl. Polym. Sci.* **2010**, *118*, 2195−2201.
(37) Lange, R. F. M.; Meijer, E. W. Supramolecular polymer interactions based on the alternating copolymer of styrene and Maleimide. *Macromolecules* **1995**, *28*, 782−783.
(38) Chee, S. S.; Jawaid, M.; Sultan, M. T. H. Thermal stability and dynamic mechanical properties of kenaf/bamboo fibre reinforced epoxy composites. *BioResources* **2017**, *12*, 7118−7132.
(39) Hirsch, C.; Striegl, B.; Mathes, S.; Adlhart, C.; Edelmann, M.; Bono, E.; Gaan, S.; Salmeia, K. A.; Hoelting, L.; Krebs, A.; et al. Multiparameter toxicity assessment of novel DOPO-derived organophosphorus flame retardants. *Arch. Toxicol.* **2017**, *91*, 407−425.
(40) Gérard, C.; Fontaine, G.; Bellayer, S.; Bourbigot, S. Reaction to fire of an intumescent epoxy resin: Protection mechanisms and synergy. *Polym. Degrad. Stab.* **2012**, *97*, 1366−1386.
(41) Salmeia, K. A.; Gaan, S. An overview of some recent advances in DOPO-derivatives: Chemistry and flame retardant applications. *Polym. Degrad. Stab.* **2015**, *113*, 119−134.
(42) Zhan, G.; Zhang, L.; Tao, Y.; Wang, Y.; Zhu, X.; Li, D. Anodic ammonia oxidation to nitrogen gas catalyzed by mixed biofilms in bioelectrochemical systems. *Electrochim. Acta* **2014**, *135*, 345−350.
(43) Li, Q.; Jiang, P.; Su, Z.; Wei, P.; Wang, G.; Tang, X. Synergistic effect of phosphorus, nitrogen, and silicon on flame-retardant properties and char yield in polypropylene. *J. Appl. Polym. Sci.* **2005**, *96*, 854−860.
(44) Lyon, R. E. *Fire Response of Geopolymer Structural Composites*; Federal Aviation Administration Washington DC Office of Aviation Research, 1996. http://www.tc.faa.gov/its/worldpac/techrpt/artn9522.pdf (accessed Sept 22, 2021).
(45) Karlsson, B.; Magnusson, S. E. Combustible wall lining materials: Numerical simulation of room fire growth and the outline

https://doi.org/10.1021/acsapm.1c01240
ACS Appl. Polym. Mater. 2021, 3, 5969−5981

of a reliability based classification procedure. *Fire Saf. Sci.* **1991**, *3*, 667−678.
(46) Lyon, R. E.; Balaguru, P. N.; Foden, A.; Sorathia, U.; Davidovits, J.; Davidovics, M. Fire-resistant aluminosilicate composites. *Fire Mater.* **1997**, *21*, 67−73.
(47) Mukai, H.; Ambe, Y. Characterization of a humic acid-like brown substance in airborne particulate matter and tentative identification of its origin. *Atmos. Environ.* **1986**, *20*, 813−819.
(48) Bifulco, A.; Marotta, A.; Passaro, J.; Costantini, A.; Cerruti, P.; Gentile, G.; Ambrogi, V.; Malucelli, G.; Branda, F. Thermal and fire behavior of a bio-based epoxy/silica hybrid cured with methyl nadic anhydride. *Polymers* **2020**, *12*, 1661.
(49) Jian, R.; Wang, P.; Duan, W.; Wang, J.; Zheng, X.; Weng, J. Synthesis of a novel P/N/S-containing flame retardant and its application in epoxy resin: thermal property, flame retardance, and pyrolysis behavior. *Ind. Eng. Chem. Res.* **2016**, *55*, 11520−11527.
(50) Gooneie, A.; Simonetti, P.; Salmeia, K. A.; Gaan, S.; Hufenus, R.; Heuberger, M. P. Enhanced PET processing with organophosphorus additive: Flame retardant products with added-value for recycling. *Polym. Degrad. Stab.* **2019**, *160*, 218−228.
(51) Matějka, L.; Dukh, O.; Kolařík, J. Reinforcement of crosslinked rubbery epoxies by in-situ formed silica. *Polymer* **2000**, *41*, 1449−1459.
(52) Molyneux, S.; Stec, A. A.; Hull, T. R. The effect of gas phase flame retardants on fire effluent toxicity. *Polym. Degrad. Stab.* **2014**, *106*, 36−46.
(53) Yan, H.; Lu, C.; Jing, D.; Hou, X. Chemical degradation of TGDDM/DDS epoxy resin in supercritical 1-propanol: Promotion effect of hydrogenation on thermolysis. *Polym. Degrad. Stab.* **2013**, *98*, 2571−2582.
(54) Musto, P. Two-Dimensional FTIR spectroscopy studies on the thermal-oxidative degradation of epoxy and epoxy− bis (maleimide) networks. *Macromolecules* **2003**, *36*, 3210−3221.
(55) Sha, L.; Chen, K. Preparation and characterization of ammonium polyphosphate/diatomite composite fillers and assessment of their flame-retardant effects on paper. *BioResources* **2014**, *9*, 3104−3116.
(56) Dittrich, B.; Wartig, K.-A.; Mülhaupt, R.; Schartel, B. Flame-retardancy properties of intumescent ammonium poly (phosphate) and mineral filler magnesium hydroxide in combination with graphene. *Polymers* **2014**, *6*, 2875−2895.
(57) Schartel, B. Phosphorus-based Flame Retardancy Mechanisms—Old Hat or a Starting Point for Future Development? *Materials* **2010**, *3*, 4710−4745.
(58) Maqsood, M.; Seide, G. Investigation of the Flammability and Thermal Stability of Halogen-Free Intumescent System in Biopolymer Composites Containing Biobased Carbonization Agent and Mechanism of Their Char Formation. *Polymers* **2019**, *11*, No. 48.
(59) Hörold, S. Phosphorus flame retardants in thermoset resins. *Polym. Degrad. Stab.* **1999**, *64*, 427−431.
(60) Visakh, P. M.; Yoshihiko, A. Flame Retardants: Polymer Blends, Composites and Nanocomposites. In *Flame Retardancy of Polymer Nanocomposite*; Springer: Cham, 2015; Chapter 2, pp 15−44.
(61) Yim, S. D.; Kim, S. J.; Baik, J. H.; Nam, I. S.; Mok, Y. S.; Lee, J.-H.; Cho, B. K.; Oh, S. H. Decomposition of urea into NH3 for the SCR process. *Ind. Eng. Chem. Res.* **2004**, *43*, 4856−4863.
(62) Gilman, J. W.; Harris, R. H., Jr.; Shields, J. R.; Kashiwagi, T.; Morgan, A. B. A study of the flammability reduction mechanism of polystyrene-layered silicate nanocomposite: layered silicate reinforced carbonaceous char. *Polym. Adv. Technol.* **2006**, *17*, 263−271.
(63) Dong, Q.; Liu, M.; Ding, Y.; Wang, F.; Gao, C.; Liu, P.; Wen, B.; Zhang, S.; Yang, M. Synergistic effect of DOPO immobilized silica nanoparticles in the intumescent flame retarded polypropylene composites. *Polym. Adv. Technol.* **2013**, *24*, 732−739.
(64) Cozza, R. C.; Verma, V. Evaluation of fracture toughness of epoxy polymer composite incorporating micro/nano silica, rubber and CNTs. *Polímeros* **2020**, *30*, No. e2020030.
(65) Rad, E. R.; Vahabi, H.; de Anda, A. R.; Saeb, M. R.; Thomas, S. Bio-epoxy resins with inherent flame retardancy. *Prog. Org. Coat.* **2019**, *135*, 608−612.
(66) Ma, S.; Liu, X.; Jiang, Y.; Fan, L.; Feng, J.; Zhu, J. Synthesis and properties of phosphorus-containing bio-based epoxy resin from itaconic acid. *Sci. China: Chem.* **2014**, *57*, 379−388.
(67) Chang, Q.; Long, L.; He, W.; Qin, S.; Yu, J. Thermal degradation behavior of PLA composites containing bis DOPO phosphonates. *Thermochim. Acta* **2016**, *639*, 84−90.
(68) Yan, W.; Yu, J.; Zhang, M.; Wang, T.; Wen, C.; Qin, S.; Huang, W. Effect of multiwalled carbon nanotubes and phenethyl-bridged DOPO derivative on flame retardancy of epoxy resin. *J. Polym. Res.* **2018**, *25*, No. 72.
(69) Yan, W.; Wang, K.; Huang, W.; Wang, M.; Wang, T.; Tu, C.; Tian, Q. Synergistic effects of phenethyl-bridged DOPO derivative with Al (OH) 3 on flame retardancy for epoxy resins. *Polym.-Plast. Technol. Mater.* **2020**, *59*, 797−808.
(70) Rakotomalala, M.; Wagner, S.; Döring, M. Recent developments in halogen free flame retardants for epoxy resins for electrical and electronic applications. *Materials* **2010**, *3*, 4300−4327.

https://doi.org/10.1021/acsapm.1c01240
ACS Appl. Polym. Mater. 2021, 3, 5969−5981